PERGAMON

International Journal of Heat and Mass Transfer 45 (2002) 201–211

International Journal of HEAT and MASS TRANSFER

www.elsevier.com/locate/ijhmt

Augmentation of heat transfer during filmwise condensation of steam and R-134a over single horizontal finned tubes

Ravi Kumar [a,*], H.K. Varma [b], Bikash Mohanty [c], K.N. Agrawal [d]

[a] *Mechanical Engineering Group, Birla Institute of Technology & Science, Pilani 333 031, India*
[b] *Mechanical Engineering Department, AKG Engineering College, Ghaziabad 201 001, India*
[c] *Chemical Engineering Department, University of Roorkee, Roorkee 247 667, India*
[d] *Mechanical & Industrial Engineering Department, University of Roorkee, Roorkee 247 667, India*

Received 25 December 1998

Abstract

An experimental investigation has been carried out to augment the heat transfer rate by enhancing the heat transfer coefficient during the condensation of pure vapours of steam and R-134a over horizontal finned tubes. The study was conducted for plain tubes, circular integral-fin tubes (CIFTs), spine integral-fin tubes (SIFTs) and parially spined circular integral-fin tubes (PCIFTs). The SIFT out performed the CIFT for the condensation of R-134a by approximately 16%. However, the spines were found most effective in the bottom side of the CIFT. The PCIFTs with the spines only in the bottom side of the tube augmented the heat transfer coefficient by 20% and 11% for the condensation of steam and R-134a, respectively, in comparison to the CIFT.

1. Introduction

It has been observed by many investigators that the heat transfer coefficient during filmwise condensation of pure vapours over a horizontal tube can be increased many folds by providing circular fins on the outer surface of the tube [1–3]. The enhancement in heat transfer coefficient by the circular integral-fin tube (CIFT) has been found to be much more than the increase in the tube surface area due to finning [4,5]. In the filmwise condensation, the curvature of the condensate film changes from top of the fin to the root of the fin on the tube surface. Hence, the surface tension of condensate causes a resultant force on the condensate film towards the root of the fin, which results in the reduction of the condensate film thickness on the fin surface. The thinning of condensate film on the fin surface causes the augmentation of condensing side heat transfer coefficient more than the increase in tube surface area due to finning. It has been observed that for the condensation of steam, a CIFT with 390 fpm fin density of rectangular fins and 1.5 mm fin spacing can augment the heat transfer coefficient by 2.5–3.0 folds [4]. However, the optimum fin density for the condensation of R-11 is 1417 fpm [5]. With this fin density the heat transfer coefficient for the condensation of R-11 can be augmented by approximately 10 folds. Similarly, for the condensation of R-134a the optimum fin density has been found to be 1560 fpm [6]. The refrigerant R-134a is an environment friendly substitute of R-12 [7]. The use of R-12 has been banned owing to its ozone depletion tendency.

It has also been reported that the heat transfer coefficient at the optimum fin density can further be enhanced by cutting several axial slots on the finned tube surface [5,8]. The depth of the slots remains equal to the fin height. In fact, cutting of slots on the CIFT surface will generate spines on the tube surface. These spines have been found to further improve the performance of a CIFT with optimum fin density. For the condensation of steam and R-11 the spine integral-fin tube (SIFT) has improved the performance of a CIFT with optimum fin density by approximately 30% [8] and 20%, respectively, [5].

Such type of study for the condensation of R-134a over a SIFT has not been carried out. The better

* Corresponding author. Tel.: +91-1596-45073 ext. 225; fax: +91-1596-44183.
E-mail address: ravi@bits-pilani.ac.in (R. Kumar).

0017-9310/02/$ - see front matter
PII: S0017-9310(01)00128-4

Nomenclature

D_i	inside diameter of test-section (m)
D_o	outside diameter of test-section (m)
D_r	fin root diameter of test-section (m)
ef	fin height (m)
es	spine height (m)
EF	enhancement factor
h_{Nu}	heat transfer coefficient by the Nusselt model (kW/m^2 K)
h_o	condensing side heat transfer coefficient (kW/m^2 K)
k	thermal conductivity of condensate (kW/m K)
L	length of test-section (m)
P_f	fin pitch (m)
P_{fc}	circular pitch of spine (m)
q	heat flux (kW/m^2)
R_p	h_o/h_{Nu} for a plain tube
tb	fin thickness at fin bottom (m)
tt	fin thickness at fin top (m)
tt_b	thickness of spine at bottom (m)
tt_c	thickness of spine at top (m)
T_s	saturation temperature of the vapour (K)
T_{wo}	test-section outside wall temperature (at fin root diameter for finned tubes) (K)

Greek symbols

ρ	condensate density (kg/m^3)
σ	surface tension of condensate (Pa m)
θ	semi-vertex angle of fin (°)
θ_c	semi-vertex angle of spine (°)
μ	viscosity (Pa s)
ΔT_f	temperature difference across the condensate layer, $(T_s - T_{wo})$ (K)
λ	latent heat of vaporization (kJ/kg)

performance of SIFTs over CIFTs is attributed to two factors. First, in SIFTs the condensate film on the fin surface is pulled down in two directions thereby thinning of condensate film on the tube surface [5]. Second, the faster condensate drainage capacity of the spine fins on the bottom of the horizontal tube [9]. The relative presence of these two factors in the better performance of SIFT had yet to be known.

The present investigation was done to compare the relative performance of SIFTs and CIFTs for the condensation of R-134a. Further investigations were also carried out to find the position of the tube surface where the fins are more effective, i.e. upper half of the horizontal tube surface or the lower half of the horizontal tube surface, for the condensation of steam (a high surface tension fluid and R-134a (a low surface tension fluid).

2. Experimental set-up and procedure

The experiments for the condensation of steam and refrigerants (R-12 and R-134a) were conducted on two different experimental set-ups one each for steam and refrigerants.

2.1. Condensation of steam

The experimental set-up to acquire data for the condensation of steam over a horizontal tube has been shown in Fig. 1. The set-up primarily consisted a test-section (9) fixed inside the test-condenser (5). The cooling water from water tank (3) was circulated inside the test-section with the help of a centrifugal pump (18) installed between the cooling water tank (3) and the test-condenser. The rotameters (12) were fixed after the centrifugal pump to measure the cooling water flow rate inside the test-section. The hot water emerging from the test-condenser was collected in the hot water tank (20) and subsequently it was sent to the drain via valve V16.

The steam which was supplied to the test-condenser, was generated in an oil fired boiler. The pressure of steam supplied from the boiler was reduced to the desired level by a pressure regulator (1). The valve V3 was provided to meet the fine adjustment of steam pressure. An auxiliary condenser (11) was also provided to condense the excess steam and remove the non-condensable. In the auxiliary condenser the condensate was removed via valve V17. Approximately 20% of the total steam was condensed inside the auxiliary condenser.

The pressure of steam inside the test-condenser was measured with the help of a pressure gauge (4). In order to measure the test-section tube wall temperature, 32 SWG teflon coated copper-constantant thermocouples were fixed on the test-section tube wall at the top side and bottom positions. The dividing plane was perpendicular to the axis of the tube. The temperature of the steam was measured by two thermocouples fixed 15 mm above and 15 mm below the test-section. The cooling water inlet and outlet temperatures were also measured by the copper-constantant thermocouples. Before installation, the thermocouples were calibrated for an accuracy of 0.1°C. Before data acquisition the experimental set-up was tested for any leakage at 300 kPa gauge pressure and 300 mm Hg vacuum.

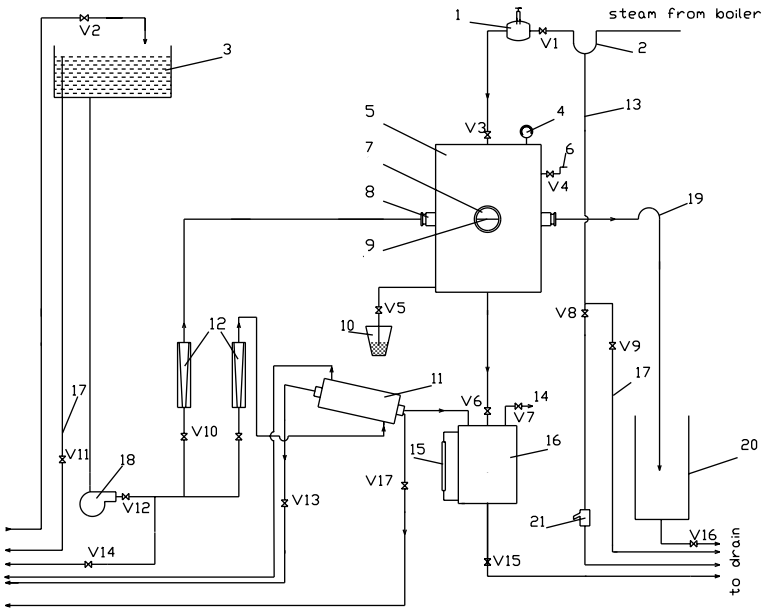

Fig. 1. Schematic diagram of experimental set-up for the condensation of steam.

Prior to supplying steam to the test-condenser it was passed through the condensate drainage pipe (13) and valve V9 for 30 min to remove all rust and dirt particles from the steam pipe line. The steam entered the test-condenser through the valve V3. The condensate from the test-section was collected in an inclined tray and was subsequently removed through valve V5. The non-condensable traces present in the experimental set-up were removed as detailed in [8].

Table 1 shows the dimensions of test-section used in this investigation and their geometry in Fig. 2. All the test-sections were made out of the copper tube. The length of the test-sections for the condensation of steam and R-134a was 310 and 417 mm, respectively. The cooling water flow rate was varied from 480 to 1680 kg/h in five steps. The gauge pressure of the condensing steam was also varied from 10 to 110 kPa in five steps for each cooling water flow rate. Therefore, for each tube 36 test runs were conducted. First, the data were acquired for the condensation over a plain tube. The results were used to establish the integrity of the experimental set-up and to have reference data to compare the performance of finned tubes. The plain tube was replaced by CIFT-1 followed by SIFT-1. The SIFT-1 was manufactured by cutting 40 axial slots on the surface of CIFT-1. The depth of slots was nearly equal to the fin height. Two partially spined circular integral-fin tubes (PCIFTs) were also manufactured by cutting 20 axial slots on the upper half of the tube surface, i.e. PCIFT-1 and 20 axial slots on the lower half of the tube surface, i.e. PCIFT-2. In both cases the dividing plane passed through the axis of the test-section.

2.2. Condensation of refrigerants

The study of condensation of R-134a was carried out on the experimental set-up shown in Fig. 3. Since the R-134a is a new refrigerant, the data were first acquired for the condensation of a refrigerant with known thermal behaviour, i.e. R-12 over a plain tube to establish the integrity of the experimental set-up. Later on, the R-12 was replaced by the R-134a and the data were acquired for the investigation on the plain tube and different finned tubes.

The vapour of R-134a was generated in the evaporator (6) with the help of three immersion heaters (5) of 3 kW each, submerged in the pool of liquid refrigerant. To check the level of the refrigerant inside the evaporator a level indicator (4) was provided with the evaporator. The heating rate of the liquid refrigerant was controlled by a variac. A pressure gauge (7) was fixed in the evaporator to avoid any disproportionate pressure rise inside the evaporator.

The evaporator was connected to the test-condenser (15) by a copper pipe of 19 mm diameter. The test-condenser was a mild steel cylinder of 100 mm diameter and 415 mm length. Inside the test-condenser the test-section (12) was fixed. The vapour of refrigerant was distributed inside the test-condenser through a dead end pipe of 350 mm length and 6.5 mm diameter. At the bottom of test-condenser two receiver valves V14 and V15 were fixed to remove the condensate from the test-condenser. A pressure-gauge (13) was also installed to measure the pressure inside the test-condenser. The excess vapour inside the test-condenser was removed by

Table 1
Gometry of test section-tubes and of spines on the circumference of SIFTs and PCIFTs

Fluid	Tube-no	Tube type	Fin density (fpm)	D_o (mm)	D_r (mm)	P_f (mm)	tt (mm)	tb (m)	ef (mm)	θ (°)
Gometry of test section-tubes										
Steam	Tube-1	Plain tube	–	22.10	–	–	–	–	–	–
	Tube-2	CIFT-1	390	24.97	22.77	2.57	1.11	1.11	1.10	0
	Tube-3	SIFT-1	390	24.98	22.87	2.56	1.11	1.11	1.06	0
	Tube-4	PCIFT-1	390	24.94	23.03	2.58	1.15	1.15	0.96	0
	Tube-5	PCIFT-2	390	24.94	23.03	2.58	1.15	1.15	0.96	0
R-12	Tube-6	Plain tube	–	21.35	–	–	–	–	–	–
R-134a	Tube-7	Plain tube	–	21.35	–	–	–	–		–
	Tube-8	CIFT-2	1560	24.68	23.08	0.63	0.10	0.52	0.80	15
	Tube-9	SIFT-2	1560	24.18	22.62	0.64	0.11	0.53	0.78	15
	Tube-10	PCIFT-3	1560	23.62	22.10	0.63	0.10	0.51	0.76	15
	Tube-11	PCIFT-4	1560	23.62	22.10	0.63	0.10	0.51	0.76	15
Fluid	Tube no.	Tube type	p_{fc} (mm)	tt_c (mm)	tb_c (mm)	es (mm)	θ_c (°)			
Geometry of spines on the circumference of SIFTs and PCIFTs										
Steam	Tube-3	SIFT-1	1.97	1.07	1.07	0.93	0			
	Tube-4	PCIFT-1	1.96	1.04	1.04	0.89	0			
	Tube-5	PCIFT-2	1.96	1.04	1.04	0.89	0			
R-134a	Tube-9	SIFT-2	1.27	0.58	1.13	0.68	22.5			
	Tube-10	PCIFT-3	1.24	0.59	1.11	0.66	22.5			
	Tube-11	PCIFT-4	1.24	0.59	1.11	0.66	22.5			

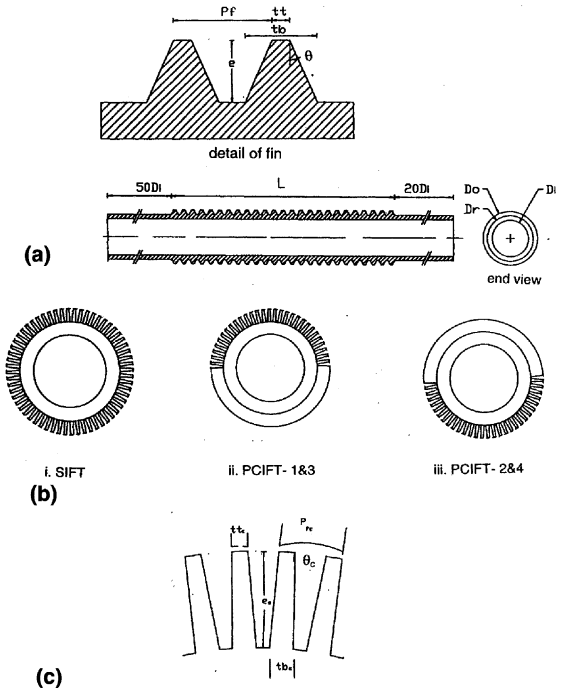

Fig. 2. Test-section geometry: (a) details of a circular integral fin tube; (b) end views; (c) spine.

the valve V13 connected to the auxiliary condenser (10). The auxiliary condenser was a horizontal cylinder of 100 mm inside diameter and 150 mm length. The water was circulated inside the auxiliary condenser through a copper tube to condense residual vapour flowing out from the test-condenser. The condensate from the auxiliary condenser was returned to the evaporator via valve V16.

The cooling water inside the test-condenser and the auxiliary condenser was circulated by the centrifugal pump (2). After the centrifugal pump the rotameters (3) were fixed to measure the cooling water flow rate. The test-section surface temperature was measured with the help of 36 SWG teflon coated copper constantant thermocouples. The thermocouples were fixed on the test-section surface in the similar manner as in the case of steam. The cooling water temperature rise was measured with the help of a thermopile of four copper-constantant thermocouples. The temperature of condensing vapour was measured with the help of two thermocouples. One was fixed 15 mm above the test-section and another was fixed 15 mm below the test-section. Prior to the data acquisition the experimental set-up was tested at 2 MPa gauge pressure and 600 mm Hg vacuum.

First the data were acquired for the condensation of R-12 over a plain tube. The R-12 was replaced by the R-134a and the data were acquired on the same plain tube. The plain tube was replaced by different finned tubes one

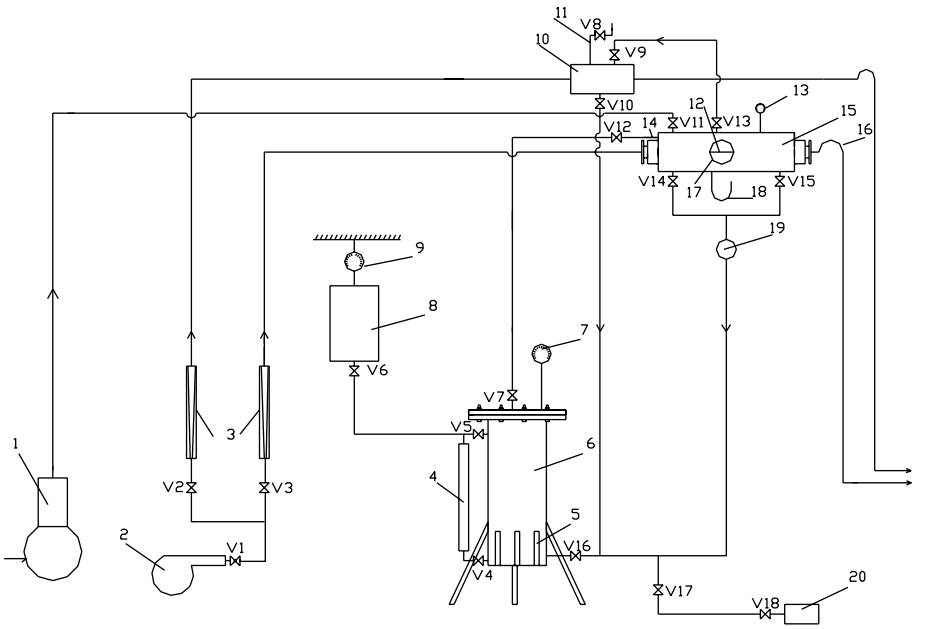

Fig. 3. Schematic diagram of experimental set-up for the condensation of refrigerants.

by one. The details of test-section are shown in Table 1. In fact, the plain tube was replaced by the CIFT-2 which has the optimum fin density of 1560 fpm [6] followed by the SIFT-2. The SIFT-2 was manufactured by cutting 60 axial slots on the surface of CIFT-2. Later, PCIFT-3 and PCIFT-4 were fixed one by one. The PCIFT-3 was manufactured by cutting 30 axial slots on the upper half of the horizontal CIFT-2 and PCIFT-4 was manufactured by cutting 30 axial slots on the lower half of the horizontal CIFT-2. The dividing plane passed through the axis of the tube. The temperature of condensing vapour of R-134a was 312 ± 0.5 K and the cooling water flow rate was changed from 400 to 1050 kg/h in the steps of 50 kg/h. Each tube was investigated for the 14 test runs. Hence, in the experimental set-up shown in Fig. 3, all together, 84 test runs were conducted.

The cooling water flow rate was measured with the help of rotameters and all the temperatures were measured by copper constantant thermocouples. The the rotameters were calibrated for an accuracy of 0.25 lpm flow rate for the condensation of steam and 20 kg/h for the condensation of R-134a in two different experimental set-ups. The thermocouples were calibrated prior to installation to an accuracy of 0.1°C. An uncertainty analysis was carried out as suggested by Kline and McClintok [10] to find out maximum possible error in the experimental results. For the condensation of steam the uncertainty in the determination of heat transfer coefficient was in the range of 2–4%. However, during condensation of R-134a the uncertainty in the heat transfer coefficient has remained in a range of 5–10%.

3. Results and discussion

The results of the investigations for the condensation of steam, R-12 and R-134a over a horizontal plain tube and the condensation of steam and R-134a over finned tubes have been discussed below.

3.1. Plain tube

The experimental condensing heat transfer coefficient for a plain tube, as obtained in this investigation was compared with that predicted by the Nusselt model [10] given by Eq. (1).

$$h_{\mathrm{Nu}} = C_{\mathrm{o}} \left(\frac{k^3 \rho^2 \mathrm{g} \lambda}{\mu D_{\mathrm{o}} \Delta T_{\mathrm{f}}} \right)^{0.25} \tag{1}$$

where the value of C_{o} for a horizontal plain tube is 0.725.

Fig. 4 illustrates a comparison of experimental heat transfer coefficient for the condensation of steam and refrigerants viz. R-12 and R-134a with that by the Nusselt model, Eq. (1). For steam, the average value of R_{p} is 1.09. This is in agreement with the findings of McAdams [12]. However, the average value of R_{p} is 0.916 for R-12 and 0.905 for R-134a. This is in agreement with the findings of White [13], who reported that the Nusselt model overpredicts the condensing side heat transfer coefficient for the condensation of R-12 by approximately 13%. If the value of constant C_{o} in the Nusselt model is modified to 0.65, the data for the condensation of R-134a and R-12 of the present

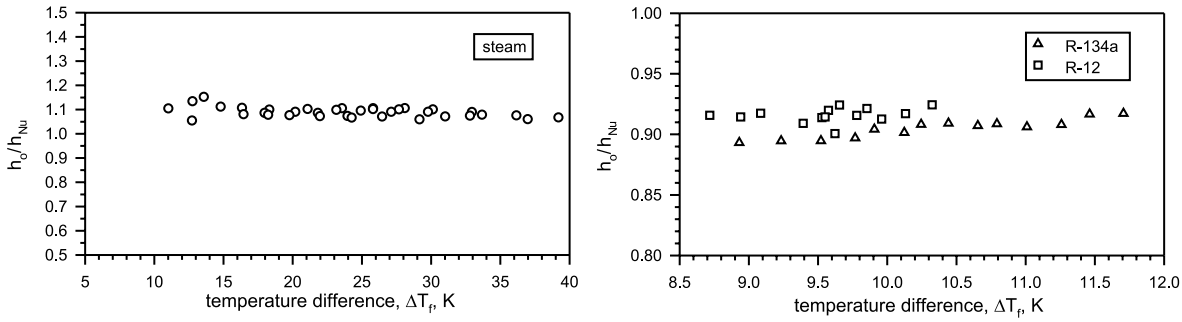

Fig. 4. Comparison between condensing side experimental heat transfer coefficient and that predicted by the Nusselt model [11] for the condensation of steam and refrigerants over a plain tube.

investigation are predicted within an error band of ±2%. Further, if the value of C_o is modified to 0.8, the heat transfer coefficient of steam from present investigation can be predicted by the Nusselt model within an error band of ±3%. The Nusselt model with modified values of C_o has been used as the modified Nusselt's model for the computation of enhancement factor, EF (ratio of heat transfer coefficient of finned tube and heat transfer coefficient of a plain tube, at same ΔT_f) of finned tubes.

3.2. Finned tubes

In Fig. 5 a graph has been plotted for the condensing heat transfer coefficient of steam on a CIFT versus ΔT_f at different T_s. It is observed in this graph that the heat transfer coefficient decreases with increase in ΔT_f at all the value of saturation temperature, T_s. Moreover, the heat transfer coefficient is not dependent on the temperature of the condensing vapour. In the range of ΔT_f from 5.3 to 23.7 K, the condensing side heat transfer coefficient lies within ±5% of the best fit line and 80% of experimental data lie in a range of ±3%. Therefore, the temperature of steam, T_s, in the given range (374–394 K) does not affect the heat transfer coefficient because the uncertainty in the determination of heat transfer coefficient also lies in the range of 2–4%.

Figs. 6 and 7 are drawn to show the variation of condensing side heat transfer coefficient of different finned tubes with respect to vapour to wall temperature difference, ΔT_f, for steam and R-134a, respectively. It is found in these graphs too, as seen in Fig. 6, that the heat transfer coefficient decreases with increase in ΔT_f for the

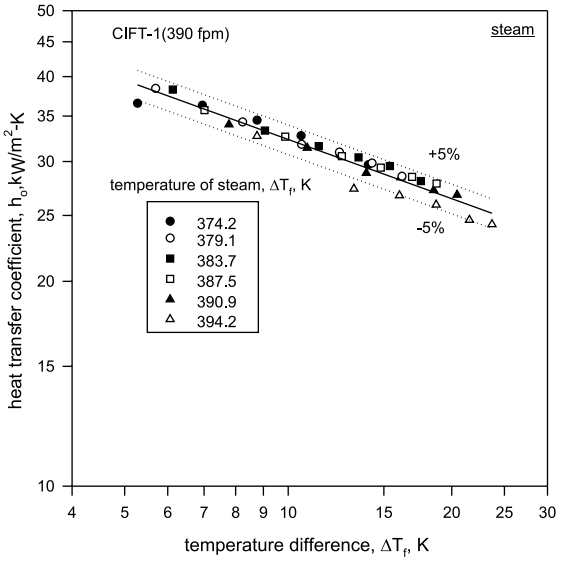

Fig. 5. Effect of the temperature of condensing vapour on condensing side heat transfer coefficient for the condensation of steam.

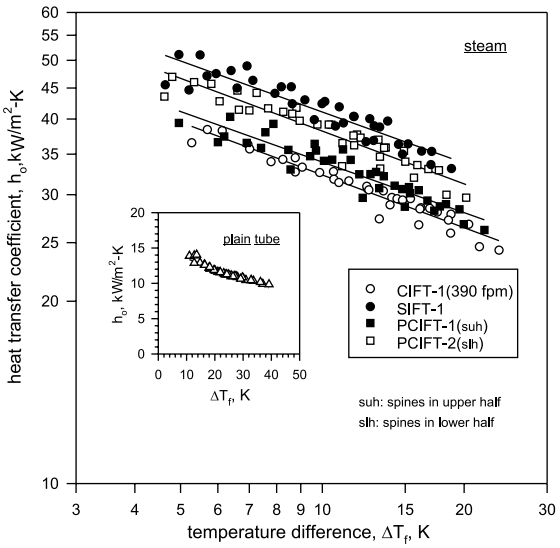

Fig. 6. Variation of condensing side experimental heat transfer coefficient with vapour to tube wall temperature difference for the condensation of steam.

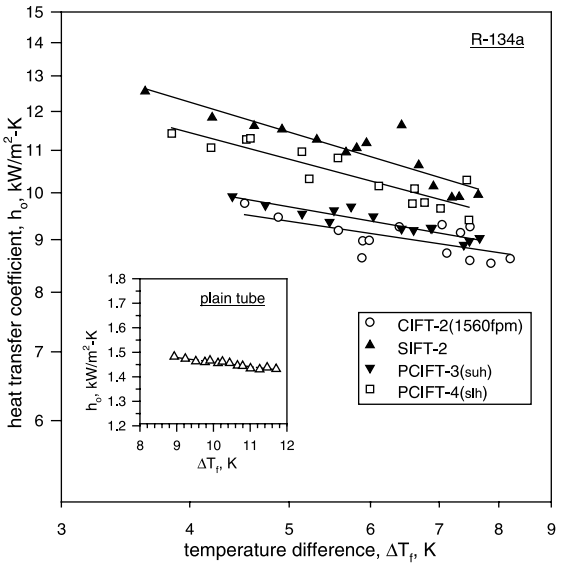

Fig. 7. Variation of condensing side experimental heat transfer coefficient with vapour to tube wall temperature difference for the condensation of R-134a.

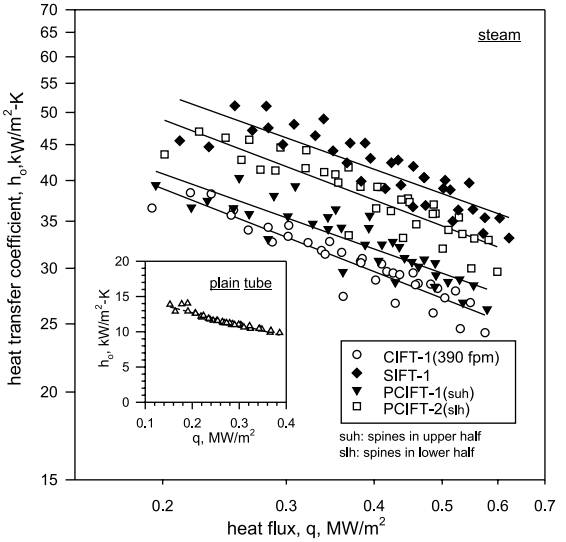

Fig. 8. Variation of condensing side experimental heat transfer coefficient with heat flux for the condensation of steam.

condensation of steam and R-134a as well. At a given ΔT_f, the heat transfer coefficient for the condensation of steam and R-134a over a SIFT is higher than that for a CIFT. It can also be envisaged from the graphs that for the condensation of R-134a the performance of SIFT-2 deteriorates faster than CIFT-2 at higher ΔT_f.

It is observed that the SIFT, i.e. SIFT-1 displays better performance than plain tube and CIFT-1 for the condensation of steam. This fact is also reported in [8]. For a constant ΔT_f the condensing side heat transfer coefficient for SIFT-1 is approximately 30% more than that of CIFT-1. Unlike in the condensation of steam, the characteristic curves for the condensation of R-134a are not parallel, Fig. 8. In fact, they tend to narrow down at the higher ΔT_f. This trend indicates that the use of SIFTs is more beneficial at the lower value of ΔT_f. As the characteristic curves for CIFT-2 and SIFT-2 are not parallel to each other. Eq. (2) has been developed to correlate the ratio of heat transfer coefficients for SIFT-2 and CIFT-2 with each other for the condensation of R-134a. The least-square method of the regression analysis was used to develop this equation.

$$\frac{(h_o)_{\text{SIFT-2}}}{(h_o)_{\text{CIFT-2}}} = 1.55\Delta T_f^{-0.16} \tag{2}$$

The observation that the heat transfer coefficient at a given ΔT_f is higher for the condensation of steam and R-134a over SIFTs is due to the fact that in SIFTs the drainage of condensate from the fin surface takes place in two directions because the spines are like pyramidical projections on the tube surface. The drainage of condensate from the fin surface is under the influence of surface tension, thus, the pull exerted on the condensate film is in two directions, which facilitates the thinning of condensate film on the test-section surface [5]. Besides this, the condensate drainage from the bottom of the tube is faster as observed during the present experimentation and also observed by Rudy and Webb [9] as well. Cumulative effect of these two factors is envisaged as the decrease in ΔT_f due to thinner condensate film on the tube surface in comparison to CIFTs. Hence, it can be concluded that the SIFTs out performs the CIFTs not only for the condensation of steam [8] but for the condensation of R-134a as well in the range of ΔT_f investigated.

The performance of PCIFTs lies between that of CIFTs and SIFTs for the condensation of steam and R-134a as well. In fact, for both the fluids, PCIFT 2&4 (spines on the lower half) outperform the PCIFT -1&3 (spines on the upper half). It is also observed that at a constant ΔT_f, the condensate drainage from the tube surface of PCIFTs is higher when the spines are kept in the downward position. The faster drainage of condensate reduces the average thickness of the condensate film on the tube surface and specially improves the thermal performance of the area which otherwise remains not as effective under condensate flooding. The spines contribute to the further thinning of condensate film on the tube surface when they are in the upper half of the tube yet the average thickness of the condensate film is higher than that of the PCIFTs with spines in the lower half of the tube. Therefore, at constant ΔT_f the heat transfer coefficient is higher for PCIFTs with spines in the lower half of the tube in comparison to the PCIFTs with spines

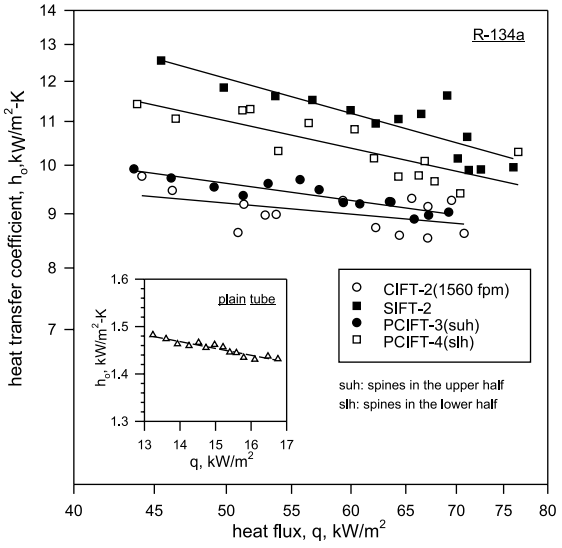

Fig. 9. Variation of condensing side experimental heat transfer coefficient with heat flux for the condensation of R-134a.

at the top of the tube for the condensation of steam and R-134a as well.

To show the variation of heat transfer coefficient with heat flux, the graphs have been plotted in Figs. 8 and 9 for steam and R-134a, respectively. These plots reveal that at a constant heat flux the condensing side heat transfer coefficient for SIFTs is more than that for CIFTs for the condensation of steam and R-134a both. Moreover, the augmentation in heat transfer coefficient by SIFT-1 is uniform for the condensation of steam for the entire range of heat flux (0.2–0.6 MW/m^2), when compared with CIFT-1. For the condensation of R-134a the performance of SIFT-2 deteriorates faster in comparison to CIFT-2 as the heat flux is increased. The SIFTs give higher heat transfer coefficient in comparison to best performing CIFT at a constant heat flux; for example, for the condensation of steam at 0.35 MW/m^2 heat flux the condensing side heat transfer coefficients for plain tube, CIFT-1 and SIFT-1 are 10.27, 31.29 and 43.51 kW/m^2 K, respectively. Hence, the SIFT enhances heat flux 4.24 times in comparison to the plain tube and 1.39 times in comparison to the CIFT-1. These values are taken from the best fit lines of the graph.

For the condensation of R-134a no generalized quantitative inference can be drawn as the characteristic curves tend to converge. At a heat flux equal to 45 kW/m^2 the heat transfer coefficient for SIFT-2 is 36% more while at the heat flux of 65 kW/m^2 the heat transfer coefficient is 24% more than that for the CIFT-2 (1560 fpm). Eq. (3) has been developed by the least-square method to correlate the ratio of heat transfer coefficients for CIFT-2 and the SIFT-2 for a given heat flux for the condensation of R-134a.

$$\frac{(h_o)_{\text{SIFT-2}}}{(h_o)_{\text{CIFT-2}}} = 3.8q^{-0.27} \tag{3}$$

At a constant heat flux the PCIFTs with spines in the lower half of the tube have higher heat transfer coefficient than those with the spines in the upper half of the tube for the condensation of steam and R-134a. For the condensation of steam at a constant heat flux of 0.35 MW/m^2 the heat transfer coefficient of the PCIFT with spines in the top position (PCIFT-1) is approximately 7% more than that of CIFT-1 and the heat transfer coefficient for PCIFT-2 (spines in the lower half) is approximately 26% more than that of CIFT-1, whereas, the heat transfer coefficient for spine fin tube (SIFT-1) is about 40% more than that of circular integral-fin tube (CIFT-1) at the same heat flux. For the condensation of R-134a the spines in the upper half of PCIFT provide only an insignificant 4% increment in heat transfer coefficient at 55 kW/m^2 heat flux when compared with the CIFT-2. This increment falls in range of uncertainty of measurements. Therefore, it cannot be safely concluded that spines are effective at the top position of the tube for the condensation of R-134a, specially at constant heat flux. When the spines are in the lower half of the tube (PCIFT-4) the increment in heat transfer coefficient at 55 kW/m^2 heat flux is about 17% of the best performing CIFT, i.e. CIFT-2. Whereas, the increment in heat transfer coefficient for SIFT-2 is 25% in comparison to CIFT-2, during condensation of R-134a.

In Figs. 10 and 11, graphs have been plotted between the enhancement factor, EF (ratio of condensing side

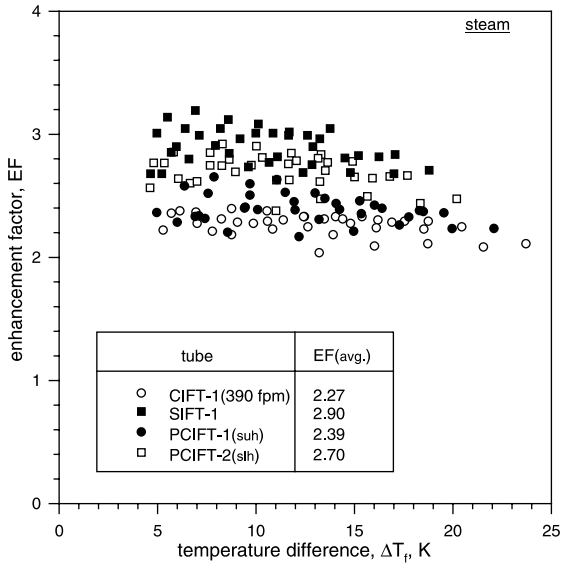

Fig. 10. Variation of enhancement factor with temperature difference across the condensate layer for the condensation of steam.

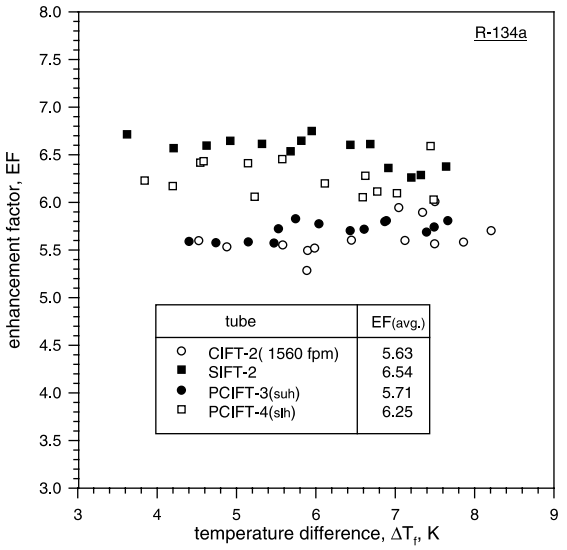

Fig. 11. Variation of enhancement factor with temperature difference across the condensate layer for the condensation of R-134a.

heat transfer coefficient and that by the modified Nusselt model at the same ΔT_f), and the vapour to tube wall temperature difference, ΔT_f, for the condensation of steam and R-134a, respectively. The average enhancement factor of SIFT-2, in Fig. 11, for the condensation of steam is approximately 30% more than that of CIFT-2, hence, confirming the superior performance of SIFT over CIFT for the condensation of steam.

The enhancement factor for SIFT becomes closer to that of CIFT for the condensation of R-134a at higher ΔT_f. In the case of refrigerant, R-134a, at 4.5 K temperature difference across the condensate film, ΔT_f, the EF for SIFT-2 is 24% more than that for CIFT-2 and at 7.5 K temperature difference, ΔT_f, the EF is only 12% more than that for CIFT-2. However, the average EF for the condensation of R-134a over SIFT-2 is approximately 16% more than that for the condensation over CIFT-2. Hence, the SIFTs are more effective for the condensation of high surface tension fluids viz. steam than the condensation of low surface tension fluids viz. R-134a. Sukhatme et al. [5] also found that the SIFTs outperform the best performing CIFT by approximately 20% for the condensation of R-11.

For the condensation of steam and R-134a the enhancement factors, EFs for PCIFTs lie between those for CIFTs and SIFTs. An investigation for the condensation of steam over PCIFTs reveals that the spines in the lower half of the tube are quite effective and the PCIFT-2 (with spines in the lower half of the tube) has enhanced the heat transfer coefficient for the condensation of steam by approximately 20%, thereby raising the EF to 2.7. For the condensation of R-134a the spines in the upper half of the tube do not seem to be effective as the EF for PCIFT-3 is only 5.71, which is marginally higher (only 1.4%) than that for the CIFT-1, i.e. 5.63. When the spines are on the bottom of the tube the EF is 6.25 for PCIFT-4, which is 11% more than that for CIFT-2.

It may be noted that the enhancement in heat transfer coefficient by SIFTs at constant ΔT_f is more than the sum of enhancement attained by the spines independently on the upper half and lower half of the tube. Although, the spines in the upper half of the tube, by themselves are not able to augment the heat transfer coefficient appreciably, yet they seem to affect the performance of spines in the lower half of the tube and over all spines on the tube surface are most effective in the improvement of the heat transfer rate for the condensation of steam and R-134a.

A comparison of the performance of CIFTs, SIFTs and PCIFTs has been made in Table 2. The spines on the upper half of the tube (PCIFT-1) are less effective for the condensation of steam and augment the EF by approximately 5% in comparison to the CIFT-1. Thus, if one can forego approximately 10% enhancement in heat transfer coefficient in comparison to SIFT-1, the use of PCIFT-2 can save about 50% of machining cost required to make a SIFT out of a CIFT. It is interesting to note from Table 2 that the percentage increase in area due to spines in SIFT-1 is approximately 10% of CIFT-1, but the EF has increased approximately 30%.

For the condensation of R-134a the spines in the top portion of the tube do no seem to be effective as these provide only 1.4% enhancement over and above CIFT-2. Therefore, spines on the bottom of the PCIFT-2 are responsible for the better performance of this tube as they improve the performance of CIFT-2 by 11%. In fact, the effect of faster drainage of condensate is more pronounced in case of R-134a, a low surface tension fluid. It can be seen in Table 2 that EFs for SIFT-2 and

Table 2
Comparison of enhancement factors of different tubes

Fluid	Tube	EF (avg.)	A_f/A_r
Steam	Plain tube	1.00	1.00
	CIFT-1 (390 fpm)	2.27	1.93
	SIFT-1	2.90	2.14
	PCIFT-1 (suh)	2.39	2.17
	PCIFT-2(slh)	2.70	2.17
R-12	Plain tube	1.00	1.00
R-134a	Plain tube	1.00	1.00
	CIFT-2 (1560 fpm)	5.63	3.06
	SIFT-2	6.54	2.31
	PCIFT-3 (suh)	5.71	2.69
	PCIFT-4 (slh)	6.25	2.69

suh: spines in upper half; slh: spines in lower half.

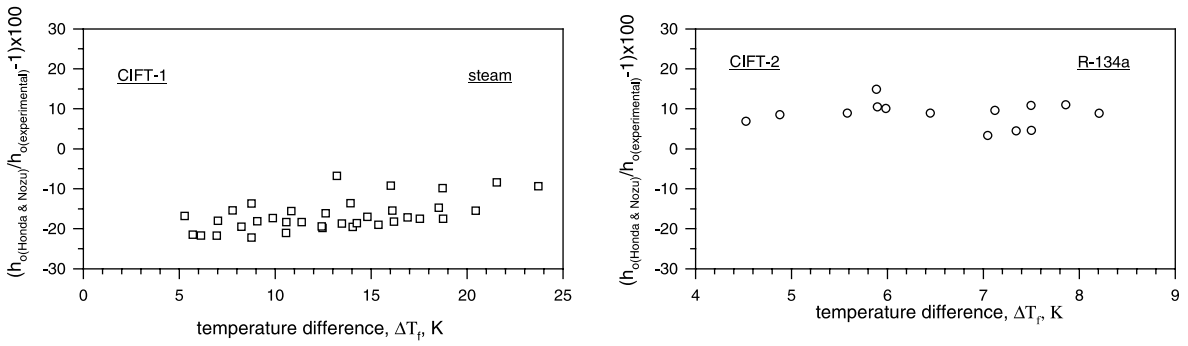

Fig. 12. Comparison of experimental heat transfer coefficient for the condensation over CIFTs with that predicted by the Honda and Nozu model [14].

PCIFT-3 are 6.53 and 6.25, respectively. Therefore, for the condensation of R-134a the spines are effective only in the lower half of the tube.

For the condensation of R-134a the area of CIFT-2 (1560 fpm) has reduced as the spines are generated on the tube surface to manufacture SIFT-2 but the average EF has increased by 16% by SIFT-2. The PCIFTs have more surface area than the SIFT-2 but the EF is less than that of SIFT-2. This clearly indicates that proper geometrical shape of the fins and its position play a deciding role in the enhancement in heat transfer coefficient.

In Fig. 12 the experimental data for the condensation over CIFTs are compared with those predicted by the Honda and Nozu model [14]. This model has predicted the experimental data for the condensation of 11 fluids over 22 different integral-fin tubes in a range of $\pm 20\%$.

4. Conclusions

1. The SIFT outperforms the CIFT with optimum fin density by 16% for the condensation of R-134a.
2. The spines are more effective in the lower half of the tubes for the condensation of steam and R-134a and improve the performance of best performing CIFT by approximately 20% for the condensation of steam and 11% for the condensation of R-134a.
3. For the condensation of R-134a the spines in the upper half of a CIFT do not contribute in the enhancement of heat transfer coefficient but shows 5% improvement in the performance of CIFT for the condensation of steam.

Acknowledgements

Authors are grateful to the Council of Scientific and Industrial Research, New Delhi, India for providing the financial assistance for the completion of this work. The authors are also thankful to the Du Pont Inc., USA for supplying a sample of R-134a to conduct the experiments.

References

[1] A.S. Wanniarachchi, P.J. Marto, J.W. Rose, Film condensation of steam on horizontal finned tubes. Effect of fin spacing, thickness and height, Multiphase Flow Heat Transfer, ASME, HTD 47 (1985) 93–99.
[2] A.S. Wanniarachchi, P.J. Marto, J.W. Rose, Film condensation of steam on finned tubes – effect of fin spacing, ASME J. Heat Transfer 108 (4) (1986) 960–966.
[3] R.L. Webb, S.T. Keswani, T.M. Rudy, Investigation of surface tension and gravity effects on film condensation, in: Proc. 7th Internat. Heat Transfer Conference, 1982, pp. 175–180.
[4] P.J. Marto, An evaluation of film condensation on horizontal integral-fin tubes, ASME J. Heat Transfer 110 (1988) 1287–1305.
[5] S.P. Sukhatme, B.S. Jagadish, P. Prabhakaran, Film condensation of R-11 vapour on single horizontal enhanced condenser tubes, ASME J. Heat Transfer 112 (1990) 229–234.
[6] R. Kumar, H.K. Varma, B. Mohanty, K.N. Agrawal, Condensation R-134a vapour over single horizontal circular integral-fin tubes, Heat Transfer Eng. 21 (2) (2000) 29–39.
[7] G.J. Epstein, S.P. Manwell, Environmental tradeoffs between CFCs and alternative refrigerants, ASHRAE J. (1992) 38–44.
[8] R. Kumar, H.K. Varma, B. Mohanty, K.N. Agrawal, Augmentation of outside tube heat transfer coefficient during condensation of steam over horizontal copper tubes, Int. Commun. Heat Mass Transfer 25 (1) (1998) 81–91.
[9] T.M. Rudy, R.L. Webb, An analytical model to predict condensate retention on horizontal integral-fin tubes, ASME J. Heat Transfer 107 (1985) 361–368.
[10] S.J. Kline, F.A. McClintock, Describing uncertaintiy in single-sample experiments, Mech. Eng. 75 (3) (1953).

[11] W. Nusselt, Die Oberflaohen-Kondensation des Wasserdampfes, VDI Zeitung, vol. 60, 1916, pp. 541–546; 569–575.
[12] W.H. McAdams, Heat Transmission, third ed., McGraw-Hill, New York.
[13] R.E. White, Condensation of refrigerant vapours apparatus and film coefficient for Freon-12, J. Soc., Refg. (1948) 375–379.
[14] H. Honda, S. Nozu, A prediction method for heat transfer during film condensation on horizontal low integral-fin tubes, ASME J. Heat Transfer 109 (1987) 218–225.